# Micro Capacitive Tilt Sensor for Human Body Movement Detection

L. Zhao, E. M. Yeatman

Optical and Semiconductor Devices Group, Department of Electrical & Electronic Engineering
Imperial College London, SW7 2AZ, UK
li.zhao@imperial.ac.uk

*Abstract*— **Tilt sensing is important for human body motion detection and measurement. Two tilt sensors are introduced in this paper, based on MEMS (Micro-electro-mechanical Systems) variable capacitors, and utilizing the gravitational effect on a suspended proof mass to detect inclinations. A symmetric comb structure with high aspect ratio is adopted to obtain high capacitance. The first device can achieve a full range (–90° to +90°) tilt angle detection and relax the high-resolution requirement of the readout system by its linear output characteristics. Based on the same concept, a novel inherently digital sensor is proposed. The digital signal can be read out without complex processing, and so low power consumption can be achieved. A fabrication process, and simulation and processing results, are presented.**

*Keywords*— **tilt sensor, comb drive, suspension beam, differential capacitance, MEMS.**

## I. Introduction

Tilt is an important parameter in many motion detection applications, including the study of human body motion, currently a topic of wide interest within biosensor design. Tracking the movement of different parts of the body can help to provide important information such as the recovery status of joint injuries, movement patterns of athletes (Fig. 1), and the sleeping patterns of insomniacs. Because tilt sensors can be highly compact, they can be combined with other motion detectors and chemical sensors, e.g. for glucose or pH, in one package, to measure physical and biochemical changes simultaneously.

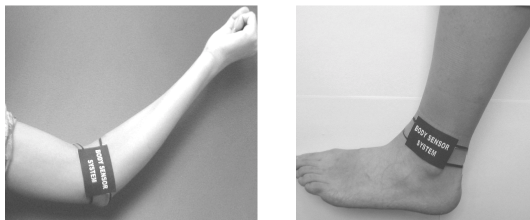


Fig 1 Examples of body movement detection; wireless sensor packs are provided at limb joints to monitor several motion parameters continuously.

Most tilt sensors reported in the literature are of capacitive type, for which we can obtain linear and analog outputs with respect to tilt angle [1]. An absolute angular encoder based on the capacitive coupling between a stator and rotor electrode has been presented in 1991 [2]. Bantien [3] invented a micromechanical tilt sensor with a moveable silicon mass mounted in a cavity using conventional micromechanical fabrication methods. This provides an alternative to conventional mercury-based sensors, avoiding the cost and toxicity inherent in mercury use. Another flat plate capacitive method for accurate angle measurement is reported in [4]. In this angle sensor, the displacement of the moveable electrode is driven by Lorentz force using a magnetic field. Changing the permittivity of the dielectric material is also a possible method for tilt angle detection [5].

While many such devices have been presented and various methods have been reported to improve their performance, the detecting range and resolution are still limited. MEMS is a good solution to extend the limitations and realize miniaturization and low cost. Although wireless body-mounted devices are the initial target, implantable variants are also a possibility, in which case minimizing size and power consumption are naturally critical requirements.

Some accelerometers can also be used as tilt sensors [6, 7]; however, the resolution is still not high enough, and the range is limited in tilt detection, due to the nonlinearity. Many accelerometers have comparatively high power consumption, which is not ideal in low power budget applications such as wireless sensor nodes. The tilt sensors introduce here are designed with low power consumption in mind.

The device fabrication is based on bonded silicon on insulator substrates, with front and back etching to release the moving parts. An inherently digital design is introduced which can simplify the read-out circuitry, or as a combined analog-digital device can maximize the range-to-resolution ratio.

## II. Device Concept

The gravity driven tilt sensor consists of a central proof mass, comb drive capacitors, and suspension beams. A 3D illustration of the device concept, as modeled in CoventorWare, is shown in Fig 2.

*L. Zhao & E.M. Yeatman, Proc.* Body Sensor Networks 2007*, Aachen, Germany, March 26-28, 2007, pp. 195-200.*

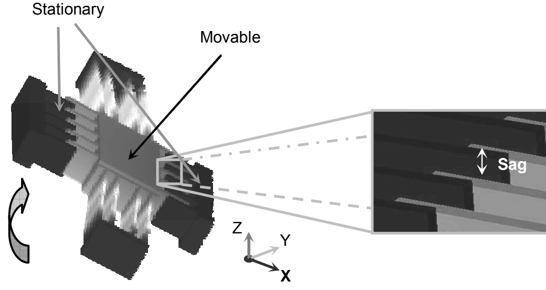


Fig 2. Operation principle of the tilt sensor.

The suspension is designed to have maximum flexibility in one in-plane direction (shown here as *x*), while being stiff in the other in-plane dimension, as well as for out-of plane motion and rotations. When tilt occurs, gravity forces the central mass to move toward one or other of the adjacent stationary comb electrodes. Hence the capacitance increases at this side, while decreasing at the other. The differential capacitance ($|C_{right}-C_{left}|$) accordingly provides a measurable parameter relating to tilt.

The comb capacitor is an efficient solution for obtaining both high capacitance and miniaturization. Operating as a displacement sensor, the key parameters of a lateral comb drive are the capacitance and lateral displacement, which are given by the following equations:

$$C = \frac{(l_o \pm \Delta x)h\varepsilon}{G} N = \frac{A_o \varepsilon}{G} N \qquad (1)$$

$$\Delta x = mg\sin(\theta)/k_x \qquad (2)$$

where C is the capacitance; $l_o$ is the initial overlap length of the finger pairs; h is the thickness of the devices; G is the width of the gap between fingers; N is the number of finger pairs; ε is the permittivity of the medium between fingers; $A_o=(l_o\pm\Delta x)h$ is the overlap area; mg is the gravitational force on the mass; $k_x$ is the spring constant in the x direction and Δx is the lateral displacement.

As can be seen, besides the characteristic suspension ($k_x$), the critical issues in achieving large capacitance variation are the aspect ratio (AR=h/G) and N. A novel etching technique described in [8] can achieve very high AR by a two step etching process. To increase the number of finger pairs, a few more sets of combs can be added without enlarging the size of the sensor.

The suspension beam design is a key issue in this sensor. Therefore, a large number of beam structures have been analysed [9, 10]. An important trade-off is that as the rigidity decreases, greater displacement (and thus greater capacitance variation) can be achieved, but the suspension will be larger, and will also allow more motion in unwanted directions, particularly sag, as shown in Fig 2.

## III. Device Structures

### *A. Initial Design*

By applying the double hammock suspension to restrict the out of plane twist and adding extra comb fingers within the body of the proof mass to increase the capacitance, we arrive at the structure shown in Fig 3(a).

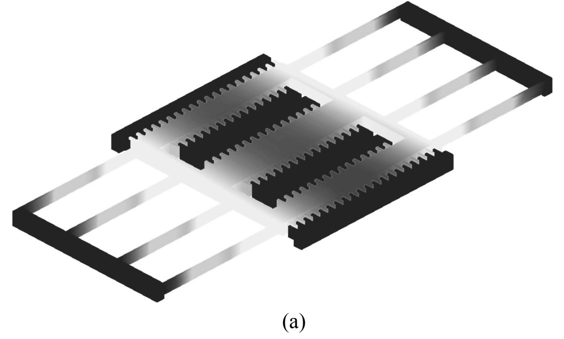

(a)

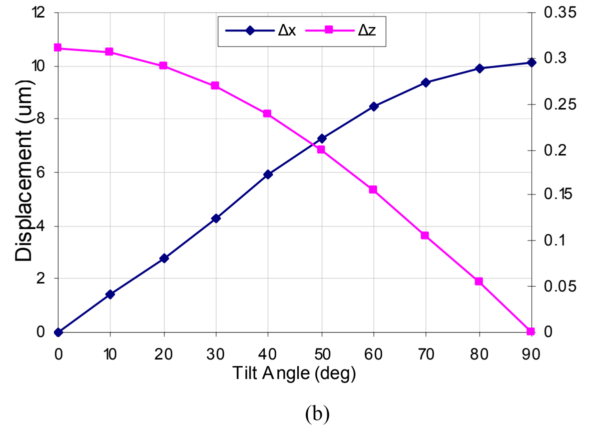


(b)

Fig 3 (a) Device design; (b) displacement in both x and z direction vs. tilt angle (the secondary axis is for Δz).

With the dimensions in Table 1, simulation results give the lateral and vertical displacements shown in Fig 3(b).

Table 1
Dimensions of the tilt sensor

| | | | |
|---|---|---|---|
| G | 2µm | w* | 2µm |
| h | 50µm | N | 250 / 208 |
| $l_0$ | 15µm | Beam | 5000×3×50µm$^3$ |
| L* | 30µm | Size | 0.25 cm$^2$×50µm |

*w denotes finger width and L is the length of the fingers.

Fig 4 shows the variation of differential capacitance ($|C_{right}-C_{left}|$) as the sensor tilt from 0° to 90°.

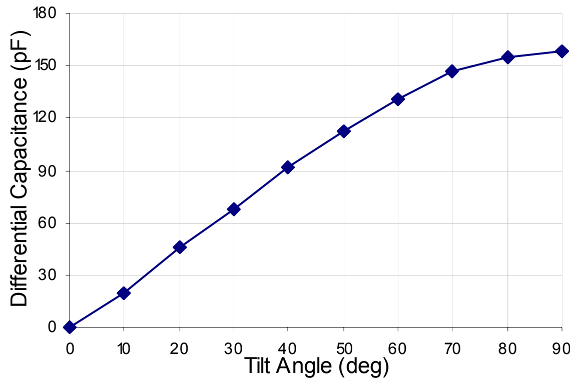


Fig 4 Relation between differential capacitance ($|C_{right}-C_{left}|$) and tilt angle.

As can be seen, the capacitance is not linearly changing with the tilt angle. This will bring complexity to the readout circuit design and cause lower resolution at large tilt angle. There are some linearization techniques which can be applied. Finger shaping is efficient to linearize the curve in Fig 4, but at the cost of lower capacitance readout. Another method is to enlarge the total sag; since the decreasing sag with tilt acts to increase capacitance as does the lateral displacement, the combined effect increases sensitivity. The summed effect gives a much more linear variation of capacitance with angle. The sag compensation has two benefits: maintenance of full resolution over the whole measurement range, and increased simplicity (and consequently reduced power consumption) of the readout circuit.

The lowest order mechanical resonant frequencies in x and z directions are 156.6 Hz and 146.9 Hz respectively. This is acceptable for body motion measurement, where a measurement bandwidth well below 100 Hz is suitable.

### *B. Digital Sensor*

MEMS variable capacitors are used in a variety of devices, such as accelerometers, to detect displacement, and in general they achieve this using a monotonic variation of capacitance across the measured displacement range. The total capacitance variation will be limited by device size and other constraints, and so the range/resolution ratio for the detector will be determined by this total variation divided by the resolution of the capacitance measurement circuit (and so ultimately by noise). However, it is possible to alter this simple range/resolution relationship by implementing a capacitance that is periodic with displacement, a technique commonly used in optical position encoders [11]. The advantage is that the rate of change of the measured quantity with displacement can be increased; however, since the measurement repeats, the output is ambiguous. This ambiguity can be resolved by having an additional reader, for example in a "coarse" and "fine" arrangement.

Using this approach we have designed a novel comb drive structure with groups of varying width finger electrodes, each group having a different width variation pattern. One possibility this allows is to directly implement a binary reader, with different periodicity of capacitance for each bit. The value of the bits can then be obtained by a simple binary comparator, either between differential capacitors or against a threshold value.

Fig 5 illustrates a 3 bit digital comb structure of this form (with only one finger per type shown for clarity). Both the moving and fixed comb fingers have periodic protrusions, and when these come into alignment the capacitance is maximised. By setting appropriate thresholds, the three bit position can be read without additional processing.

Fig 5 Schematic of a 3-bit digital comb drive.

As in the conventional design, it is important to maximise the capacitance variation. Fringing field effects will tend to "blur" the variation, and thus reduce the amplitude of the periodic capacitance change, and this effect increases as the periodicity increases (i.e. for lower order bits). However, the capacitance variation can be increased by varying the tooth-to-gap width ratio. This effect is illustrated in Fig. 6.

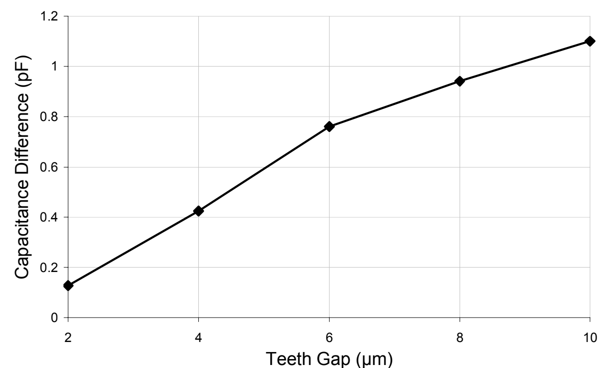


Fig 6 Capacitance variation vs. distance between teeth, for fixed tooth width of 2 μm.

The capacitance difference increases monotonically as the teeth gap width increases. However, as the gap increases, the comb fingers also have to be lengthened, and the total displacement range also increased. A large displacement range requires a large suspension, and reduces the stiffness in unwanted motion directions. Thus, a 6 μm gap width is chosen as a compromise between device size and sensitivity.

For a fully digital design, a high range/resolution ratio requires a large number of bits, and this will ultimately be limited by the minimum practical tooth width for the lowest order bit. This tooth width minimum is in turn limited by the minimum gap between fixed and moving teeth, and this depends on device stiffness as well as on fabrication precision. Meanwhile, we can still gain a resolution advantage with a combined structure as in Fig 5, by reading an analogue position from each finger type, and using the high periodicity for resolution and the low periodicity to resolve ambiguity.

## IV. FABRICATION

High thickness is desirable for the moving parts, both to maximize the proof mass and to increase out-of-plane stiffness. Electrical isolation between various elements is also needed, with low parasitic capacitance. SOI (silicon-on insulator) wafers provide a good platform for a device of this kind. Back etching is required in order to fully release the device. Therefore the sensor mechanical parts are fabricated using a two sided process, for the device layer etching and handle layer etching respectively.

### A. Device Layer Processing

Bulk machining is applied for the device layer etching. The processing flow chart is shown in Fig 7. The top silicon layer of SOI is 50 μm thick with a 1 μm thick buried oxide. Then the photoresist S1813 is spin coated and patterned by contact photolithography, and the pattern is transferred to the wafer by high aspect ratio deep reactive ion etching (DRIE).

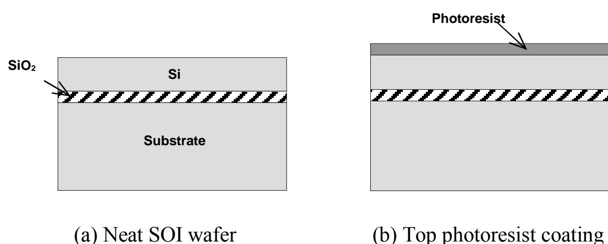


(a) Neat SOI wafer (b) Top photoresist coating

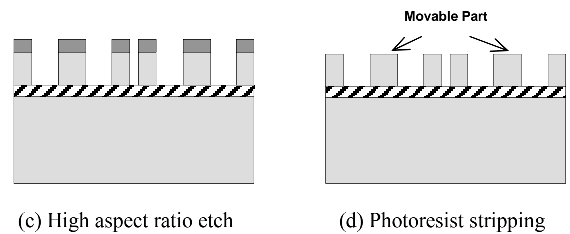


(c) High aspect ratio etch (d) Photoresist stripping

Fig 7 Device layer processing flow chart.

### B. Handle Layer Processing

The processing for device release is demanding, because there are two stationary parts in the middle of the central mass, as shown in Fig 3(a). These two parts must be electrically isolated from the movable mass, while still fixed to the substrate mechanically. Therefore, normal back etching is not acceptable here. A good solution for this problem is SCREAM (Single Crystal Reactive Etch and Metallization) processing, which is efficient to produce high aspect ratio isolated island microstructures [12, 13]. The flow chart is shown in Fig 8.

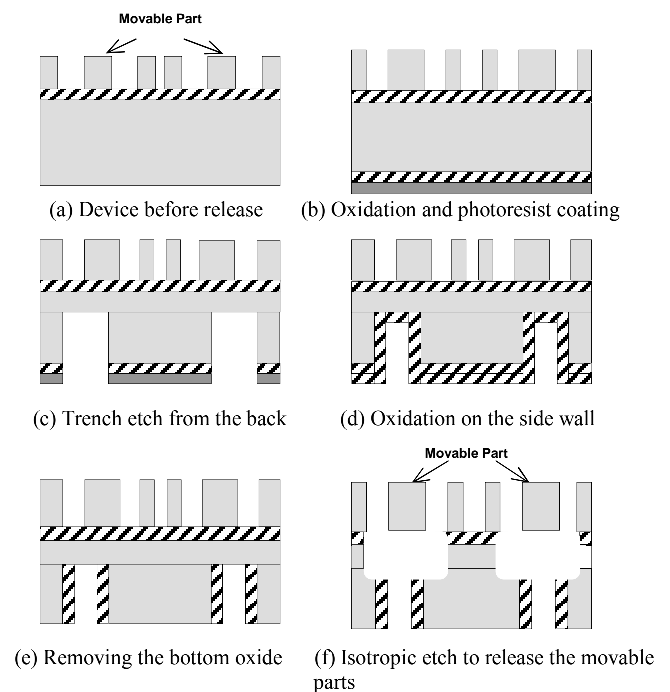


(a) Device before release (b) Oxidation and photoresist coating

(c) Trench etch from the back (d) Oxidation on the side wall

(e) Removing the bottom oxide (f) Isotropic etch to release the movable parts

Fig 8 Handle layer processing flow chart.

This part of the processing starts with anisotropic trench etching. A thick masking oxide layer must be grown at the

back of the wafer to stand the long time high aspect ratio DRIE (Fig 8(b)). After the pattern transfer to the silicon (Fig 8(c)), a new layer of oxide is grown by thermal or chemical vapor deposition to protect the side wall of the trench during the isotropic release etching (Fig 8(d)). A second mask is required to remove the silicon dioxide from the bottom of the trench (Fig 8(e)). Finally, an isotropic $SF_6$ is applied to release the movable central mass (Fig 8(f)). The released mass is suspended by the beam, which is anchored to the silicon dioxide layer of the SOI wafer, and the isolated island in the middle is supported by the substrate.

The performance of this sensor depends highly on the flatness of the sidewall etching of the comb fingers. A dry etch process has been developed for comb drive definition, giving high verticality and smooth sidewall surfaces. A fine detail of the resulting comb structure fabricated on a test wafer is shown in Fig 9. DRIE is applied for 20 minutes, and the etching depth is around 45 µm. Better features can be achieved by applying the two-step etching method described in [8].

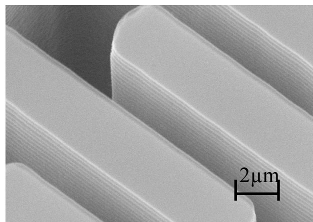


Fig 9 The SEM photo of the handle layer on a test wafer.

## V. Experiments And Results

For the periodic width finger structure, the change of the capacitance is a combination of both the periodic change in tooth alignment and the total inserted length of the moving finger. In order to separate these effects, a reference comb finger without teeth is modelled. Taking the 3rd bit as an example, the capacitance variation of 400 finger pairs is shown in Fig. 11. According to Fig 6, a 6 µm tooth gap is applied. The teeth width of the 3rd bit is 2 µm, while the widths of other bits are multiples of 2 µm.

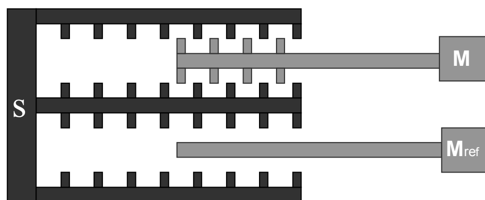


Fig 10 Digitized structure with reference finger.

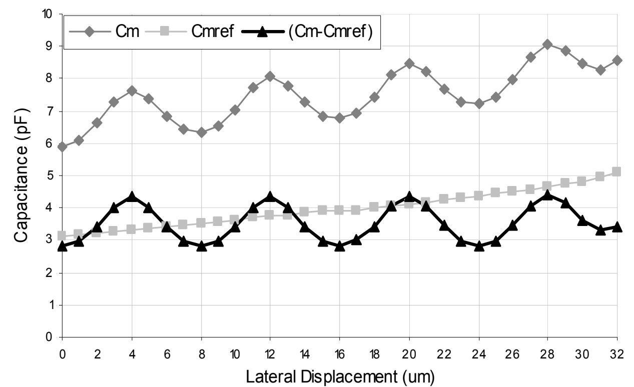


Fig 11 Capacitance variation (of 400 finger pairs) with position, for toothed and reference fingers, and the difference.

The actual capacitance read-out is ($C_M$-$C_{Mref}$). Since the lateral displacement of this sensor is large, a more flexible suspension has to be applied. For such a tilt sensor with 50 µm thickness and 400 finger pairs of each bit, the modelled relation between displacement and capacitance (simulated in CoventorWare) is shown in Fig 12, for each bit. These results show the form expected. It can be seen that for the lower order (high periodicity) bits, the capacitance contrast decreases. This is a result of the increasing effect of fringing fields

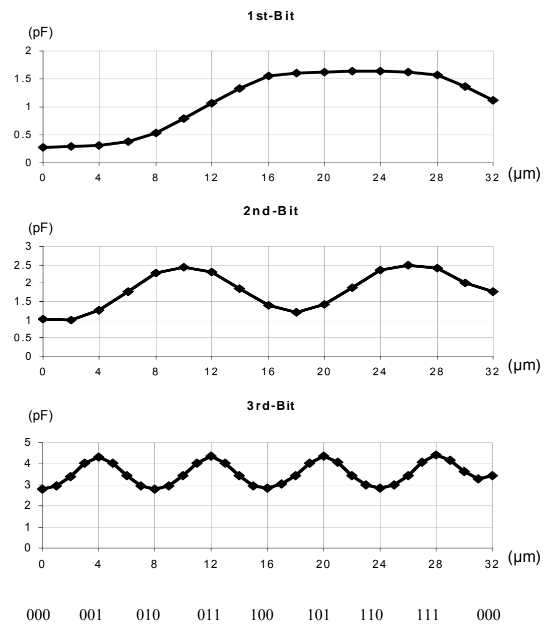


Fig 12 Output characteristic of the digital tilt sensor.

## VI. Conclusions And Discussion

A tilt sensor based on inter-digitated comb capacitors has been presented. By applying proper suspension designs, the full range of tilt angle can be accurately measured. A novel design for an inherently digital sensor is presented and analysed, which is shown to be promising in tilt angle detection. A fabrication process is described for a silicon micromachined device, and high quality finger profiles, especially the sidewalls of the fingers, are demonstrated.

Although only 3 bits are implemented in this initial device, there are still some interesting applications. One example is in patient monitoring systems. When other sensors, like heart pace detectors, are working, the information about the patient's movement, such as sleeping, walking or suddenly falling over, are also important. The resolution is less importance than low power consumption, since the whole package of sensor nodes are driven by a limited power supply.

Apart from the general applications mentioned, the tilt sensor can be used to monitor motion, and thus help to correct image distortion, in PET (Positron Emission Tomography) or computed (X-ray) tomographic scanning. Besides the clinical applications, it can also be used in bionics studies, such as robot design.

## References


[1] H.Kawamoto, "A Study of Capacitance Type Incline Sensor," *Institute of Electric and Electronics Engineering of Japan*, vol. R83-56, pp. 13-18, 1984.

[2] R. F. Wolffenbuttel and R. P. Van Kampen, "An Integrable Capacitive Angular Displacement Sensor with Improved Linearity," *Sensors and actuators. A, Physical*, vol. 27, pp. 835-843, 1991.

[3] F. Bantien, "Micromechanical Tilt Sensor." United States Patent, 1992.

[4] J. R. Kaienburg, M. Huonker, and R. Schellin, "Surface Micromachined Bridge Configurations for Accurate Angle Measurements," Micro electro mechanical systems, Miyazaki, Japan, 2000.

[5] H. Ueda, H. Ueno, K. Itoigawa, and T. Hattori, "Micro Capacitive Inclination Sensor Utilizing Dielectric Nano-Particles," IEEE, MEMS 2006, Istanbul, Turkey, 2006.

[6] A. Selvakumar and K. Najafi, "A high-sensitivity z-axis capacitive silicon microaccelerometer with a torsional suspension," *Journal of Microelectromechanical Systems*, vol. 7, pp. 192-200, 1998.

[7] J. W. Weigold, K. Najafi, and S. W. Pang, "Design and Fabrication of Submicrometer, Single Crystal Si Accelerometer," *Journal of Microelectromechanical Systems*, vol. 10, pp. 518-524, 2001.

[8] A. Lipson and E. M. Yeatman, "Free-Space MEMS tunable optical filter on (110) silicon," IEEE/LEOS International Conference on Optical MEMS and Their Applications Conference, 2005.

[9] V. P. Jaecklin, C. Linder, N. F. De Rooij, and J. M. Moret, "Micromechanical comb actuators with low driving voltage," *Journal of Micromechanics and Microengineering*, vol. 2, pp. 250, 1992.

[10] R. Legtenberg, A. W. Groeneveld, and M. Elwenspoek, "Comb-drive actuators for large displacements," *Journal of Micromechanics and Microengineering*, vol. 6, pp. 320-329, 1996.

[11] E. M. Yeatman, P. J. Kushner, and D. A. Roberts, "Use of scanned detection in optical position encoders," *IEEE Transactions on Instrumentation and Measurement*, vol. 53, pp. 37-44, 2004.

[12] G. K. Fedder, "MEMS fabrication," International Test Conference Proceedings, 2003.

[13] K. A. Shaw and N. C. MacDonald, "Integrating SCREAM micromachined devices with integrated circuits," IEEE, The Ninth Annual International Workshop on MicroElectroMechanicalSystems Proceedings, 1996.